Electrons and fractons on percolation structures at criticality: Sublocalization and superlocalization

Jan W. Kantelhardt and Armin Bunde
Institut für Theoretische Physik, Justus-Liebig-Universität Gießen, D-35392 Gießen, Germany
(Received 29 May 1997; revised manuscript received 29 August 1997)

We discuss the localization of electronic eigenfunctions and vibrational excitations (''fractons'') on self-similar percolation clusters at criticality on the Cayley tree, in $d=2$, and in $d=3$, both in topological (ℓ) and in Euclidian (r) space. We find that the localization behavior of electrons and fractons is very similar, but does depend on the type of average performed and on the number of configurations N taken into account. It can be characterized by three different localization regimes. In the first regime, at small distances ℓ and r from the localization center, electrons and fractons are superlocalized in ℓ space, while the localization is not exponential in r space. In the intermediate regime, which is the most important one, we find stretched exponential localization (''sublocalization''), $\ln\langle\psi\rangle \sim -\ell^{d_{\Psi,\ell}}$ or $\sim -r^{d_{\Psi,r}}$ with effective localization exponents $d_{\Psi,\ell} \approx d_{\Psi,r} \approx 0.6$. In the third regime, for large ℓ and r, the averages strongly depend on the number of configurations, even in ℓ space, and superlocalization ($d_{\Psi,\ell}, d_{\Psi,r} > 1$) is observed, converging to simple exponential behavior asymptotically. To understand this complicated localization behavior, we present an analytical calculation of $\ln\langle\psi\rangle$ for the third regime, which is based on the fact that the local amplitudes at large distances from the localization center obey a log-normal distribution. [S1063-651X(97)12012-8]

PACS number(s): 64.60.Cn, 71.55.Jv, 63.50.+x

I. INTRODUCTION

It is well known that in disordered structures, due to the absence of translational symmetry, electronic wave functions and vibrational excitations can be localized [1–4] i.e., their amplitudes decrease with increasing distance from a localization center for certain energies E and frequencies ω, respectively. Apart from its principal relevance, the knowledge of the localization behavior in disordered self-similar systems is relevant for a large number of both experimental and theoretical issues, ranging from the disorder-induced metal-insulator transition [3,5,6] to the thermally activated hopping conductivity in disordered systems [7–9]. A standard model for disordered systems is the percolation model [10,11]. Close to the critical concentration, self-similar structures (''fractals'') occur, and it is an open question, how the averaged eigenfunctions decay spatially on these structures and how this decay depends on the averaging procedure, especially on the number N of configurations taken into account in the average.

It is well accepted that asymptotically the mean amplitudes decay proportional to $\exp[-\text{const}\times r^{d_{\psi,r}}]$ with increasing ''air'' distance r from the localization center, but different groups report on different localization exponents $d_{\psi,r}$ [12–17]. For a ''quenched'' logarithmic average, where the fluctuations of the amplitudes $\psi_n(r)$ at site n at fixed distance r are strongly diminished by averaging over $\ln\psi_n(r)$, $d_{\psi,r}=d_{\min}$ has been predicted [16], where $d_{\min}$ is the fractal dimension of the shortest path on the percolation cluster connecting two distant points on the cluster. It has been argued that also for the arithmetic average, the value $d_{\psi,r}=d_{\min}$ should be observed in computer simulations, where by definition only few configurations can be taken into account [1,17]. If the arithmetic average is taken over *all* configurations, strict analogies between random walks and vibrational excitations suggest $d_{\psi,r}=1$ [15,10]. Most numerical calculations seem to be in accord with $d_{\psi,r}=1$ [13], while one simulation favors $d_{\psi,r}=d_{\min}$ [14].

Most previous analytical results are based on the assumption that the chemical distance ℓ from the localization center (rather than the air distance r) characterizes the localization behavior. The chemical distance (also called topological distance) between two points on a percolation cluster is defined as the shortest path distance on the cluster. Assuming that the amplitudes ψ_n at sites at fixed chemical distance ℓ from the localization center have a very narrow distribution and decay proportional to $\exp[-\text{const}\times\ell]$, the behavior of the amplitudes in ''r space'' can be derived from the behavior in ''ℓ space'' by a convolution integral, which contains the structure function of percolation clusters $\phi(\ell|r)$ [18,17,10]. The analytic treatment yields two distinct localization regimes, $d_{\Psi,r}=1$ for intermediate r $[r_1<r<r_\times(N)]$ and $d_{\Psi,r}=d_{\min}$ for large r $[r>r_\times(N)]$. Here, r_1 is of the order of the localization length λ_r, and $r_\times(N)$ increases logarithmically with N [17].

The aim of this paper is twofold: First, for checking the basic assumption of the analytical theory cited above, we study, for both electronic wave functions and vibrational excitations (''fractons'') on large percolation clusters at criticality, the distribution of the amplitudes at fixed chemical distance ℓ from the localization center, where the eigenfunctions take their maximum [19], and investigate the decay of the mean amplitudes as a function of ℓ. Then, we study the decay of the mean amplitudes as a function of the spatial distance r from the localization center. We find that the mean amplitudes of both wave functions and fractons behave quite similarly in ℓ and in r space, and we can distinguish three localization regimes:

(i) In the neighborhood of the localization center, electrons and fractons are *superlocalized* in ℓ space,

$\ln\langle\psi\rangle \sim -\ell^{d_{\Psi,\ell}}$, with $d_{\Psi,\ell} > 1$, while the localization is not exponential in r space (see also [20]).

(ii) At intermediate distances from the localization center, electrons and fractons are *sublocalized* with exponents $d_{\Psi,\ell}$ and $d_{\Psi,r}$ close to 0.6, in both ℓ and r space. This intermediate (sublocalization) regime expands logarithmically with the number of configurations N and becomes the dominant regime for large N.

(iii) In the asymptotic regime, finally, electrons and fractons are simply exponentially localized, $d_{\Psi,\ell} = d_{\Psi,r} = 1$, as expected [1,16]. For large N values, however, the crossover to the asymptotic regime occurs at extremely large distances from the localization center, which are not accessible by computer simulations.

The paper is organized as follows: In Sec. II, we introduce the basic quantities of interest and the averaging procedure we employed. In Secs. III and IV, we present our numerical results for electrons and fractons on critical percolation clusters on Cayley trees (Sec. III) as well as in $d=2$ and $d=3$ (Sec. IV). In Sec. V, finally, we use the fact that the amplitudes for fixed lengths ℓ obey a log-normal distribution to derive an analytical expression for the averaged amplitude of the wave functions at large ℓ, which becomes rigorous in the asymptotic regime. In the Appendix we briefly describe the numerical methods we employed for the calculation of the eigenfunctions.

II. MODELS AND AVERAGING PROCEDURE

We consider site percolation clusters at the critical concentration p_c, and assume that the motion of electrons can be described by hopping between nearest-neighbor cluster sites. Within the tight-binding approximation, the electronic wave function can be written as linear combination of atomic orbitals localized at the cluster sites n. The coefficients $\phi_{n,E}$ in the linear combination satisfy the time independent tight-binding equation [21,16,3]

$$E\,\phi_{n,E} = \sum_m{}' V_{n,m}\phi_{m,E}\,, \tag{1}$$

where the sum runs over all nearest-neighbor sites m of site n. The hopping terms $V_{n,m}$ are constant for nearest neighbor cluster sites and zero otherwise; for simplicity we take $V=1$ as energy unit.

The ''quantum percolation equation'' (1) is similar to the scalar vibration equation, where we assume that each cluster site has a unit mass, and nearest-neighbor sites n and m are coupled by a (scalar) force constant $V^{\alpha,\beta}_{n,m} = V^{\beta,\alpha}_{n,m} = V_{n,m}$. In this case, different components of displacements decouple and we obtain the same equation for all components $u_n(t)$. The ansatz $u_n(t) = u_{n,\omega}\exp(-i\omega t)$ leads to the time independent vibration equation [22,4,10]

$$\left(-\omega^2 + \sum_m{}' V_{n,m}\right) u_{n,\omega} = \sum_m{}' V_{n,m} u_{m,\omega}\,, \tag{2}$$

which up to the diagonal terms is identical to Eq. (1), if the energy eigenvalue E is replaced by $-\omega^2$. As above, we will choose $V=1$ in the following.

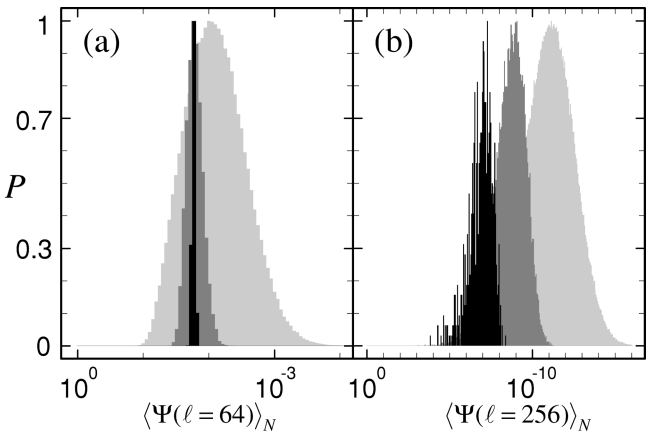

FIG. 1. Distributions P of the arithmetic averages $\langle\Psi(\ell)\rangle_N = [(1/N)\Sigma_{\nu=1}^{N}\psi^2_{(\nu)}(\ell)]^{1/2}$ for electrons on critical percolation clusters on the Cayley tree at (a) $\ell=64$ and (b) $\ell=256$ for $N=8$ (light gray), $N=128$ (dark gray), and $N=4096$ (black). The distributions have been normalized to their maximum. Evidently, the averages $\langle\Psi(\ell)\rangle_N$ depend on the number of configurations N and fluctuate strongly from one set of N configurations to the next for large ℓ.

To treat both problems simultaneously, we will introduce a function ψ_n, which stands either for the amplitude $\sqrt{\phi^*_{n,E}\phi_{n,E}}$ of the electronic wave function or for the amplitude $|u_{n,\omega}|$ of the displacement of a vibrating particle, both on a site n, for fixed E respectively ω. For convenience, we ''normalize'' ψ_n such that $\psi_n = 1$ at the localization center. By definition, the localization center is that site, where the maximum of the amplitudes occurs [19].

We are interested in a quantitative description of the way the values of ψ_n decrease with increasing distance r from the localization center. The necessary averaging procedure consists of three steps: In the first step we average, for each configuration $\nu = 1,2,\ldots,N$, the values of ψ^2_n at fixed distance r from the localization center. The resulting function $\psi^2_{(\nu)}(r)$ characterizes the spatial decrease of our quantity of interest in the considered νth cluster. In the second step, for obtaining the mean spatial decrease, we average $\psi^2_{(\nu)}(r)$ over N configurations,

$$\langle\Psi(r)\rangle_N = \sqrt{\frac{1}{N}\sum_{\nu=1}^{N}\psi^2_{(\nu)}(r)}\,. \tag{3}$$

If the system is not self-averaging (which we find is the case here), the resulting values for $\langle\Psi(r)\rangle_N$ will depend on the special set of N configurations considered and will fluctuate from set to set. An example is shown in Fig. 1, where we consider, for electrons on the Cayley tree (see Sec. III), the distribution of the values $\langle\Psi(\ell)\rangle_N$ for different sets of N configurations. Evidently, the distributions are logarithmically broad, i.e., self-averaging fails. In this case, to obtain the *typical* value of $\langle\Psi(r)\rangle_N$, we are led, in the third step, to the logarithmic average over many sets of N configurations, i.e., we average $\ln\langle\Psi(r)\rangle_N$ over many sets of N eigenfunctions [17]. The resulting function

$$\Psi_N(r) \equiv \exp\langle\ln\langle\Psi(r)\rangle_N\rangle \tag{4}$$

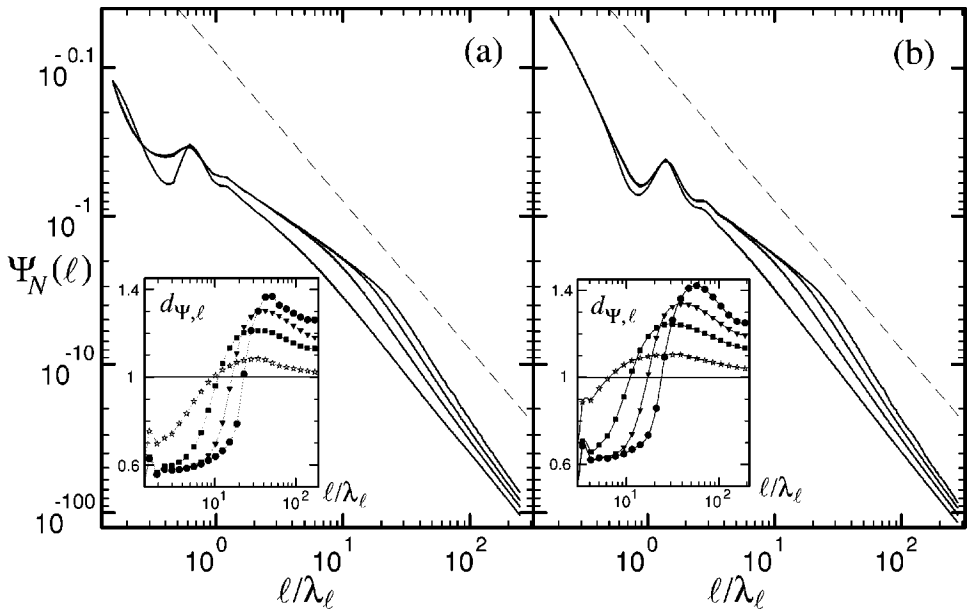

FIG. 2. Decrease of $\Psi_N(\ell) \equiv \exp\langle \ln[(1/N)\Sigma_{\nu=1}^{N} \psi_{(\nu)}^2(\ell)]/2 \rangle$ versus ℓ/λ_ℓ for (a) electrons and (b) fractons on critical percolation clusters on the Cayley tree for $N=1$ (bottom line), $N=8$, $N=128$, and $N=4096$ (top line). In all cases, 1.5×10^6 clusters of $\ell_{\max}=1200$ shells were considered in the averaging procedure. The values for λ_ℓ, (a) $\lambda_\ell=6.5$ and (b) $\lambda_\ell=5.8$, have been determined from the distributions in Fig. 4. The straight dashed lines have the slope $d_{\Psi,\ell}=1$ and are shown for comparison. In the insets, the effective local exponents $d_{\Psi,\ell}$ determined numerically from the slopes of the curves, are shown versus ℓ/λ_ℓ. The symbols correspond to the effective numbers of configurations (stars, $N=1$; squares, $N=8$; triangles, $N=128$; and circles, $N=4096$) and the lines are guides to the eye.

can be considered as the typical average. In the following, we shall discuss exclusively this ''typical average over N configurations'' defined by Eq. (4).

To characterize the localization further, we will also consider the decrease of ψ_n in ℓ space, and average ψ_n over all sites n at the topological distance ℓ from the maximum. The resulting function $\Psi_{(\nu)}(\ell)$ describes the decrease of ψ in chemical ℓ space. The average over N configurations gives $\langle \Psi(\ell) \rangle_N$ [see Eq. (3)], and we shall consider its typical value $\Psi_N(\ell)$ here [see Eq. (4)].

The question, which N should be taken for a realistic macroscopic system, depends on the quantity of interest and cannot be answered unambiguously. If, for example, one is interested in the mean electronic wave function at a given energy E or fractons of a given frequency ω in a system of N_a atoms, one averages over all N states within a certain energy or frequency ''band'' around E or ω. Clearly, N is proportional to N_a. The width of the ''band'' (and the ratio of N and N_a) will depend on the physical situation, for example on temperature or on some other parameters. Since the mean amplitudes depend sensitively on N, the results for physical quantities of interest in mesoscopic or even macroscopic systems may depend on the system size or on other parameters changing the effective N.

III. PERCOLATION CLUSTERS ON THE CAYLEY TREE

We consider percolation clusters at criticality on Cayley trees with coordination number $z=3$; the percolation threshold is $p_c=1/(z-1)=0.5$ [10]. Since the clusters have no loops, a very fast calculation of the eigenfunctions is possible (see the Appendix for details of the calculation). We have grown clusters by the Leath method [10] with a maximum chemical length $\ell_{\max}=1200$ and have calculated 2×10^6 eigenfunctions of Eqs. (1) and (2) for both electrons and fractons. Each eigenfunction was calculated on a different cluster configuration for eigenvalues $E\simeq1.7$ and $\omega^2\simeq0.1$, which were chosen to yield similar localization lengths λ_ℓ for electrons and fractons. Cayley trees cannot be embedded in space with a finite dimension, but the topological distance ℓ on the cluster structure can always be determined. Thus, we restrict ourselves to ℓ space.

Figure 2 shows $\Psi_N(\ell)$ for (a) electrons and (b) fractons for four different N values. While both electronic wave functions and fractons behave quite similarly here, the actual absolute values depend drastically on the number of configurations N included in the averaging procedure. In addition, one can see that the decay of $\Psi_N(\ell)$ is not simple exponential ($d_{\Psi,\ell}=1$) and several decay regimes with different effective exponents can be distinguished. The slopes of the curves yield the effective $d_{\Psi,\ell}$ and are shown in the insets. Since there is no self-averaging, a single value for the localization length λ_ℓ cannot be defined from the averaged eigenfunctions $\Psi_N(\ell)$. So we determined λ_ℓ from the distributions of the amplitudes ψ_n for several fixed ℓ by fitting them with a log-normal distribution as will be discussed at the end of this section. This procedure is the only way to define a unique localization length.

For $N\gg1$, we can distinguish between three different localization regimes: In the first regime, for ℓ below $\lambda_\ell/2$, we find a faster than exponential decay with an effective exponent $d_{\Psi,\ell}>1$. This regime is not shown in the insets and it is more pronounced for fractons [Fig. 2(b)]. At the end of this regime we observe some oscillations in the averaged eigenfunctions, which are the remainder of the plane wave solutions of Eqs. (1) and (2) in ordered systems.

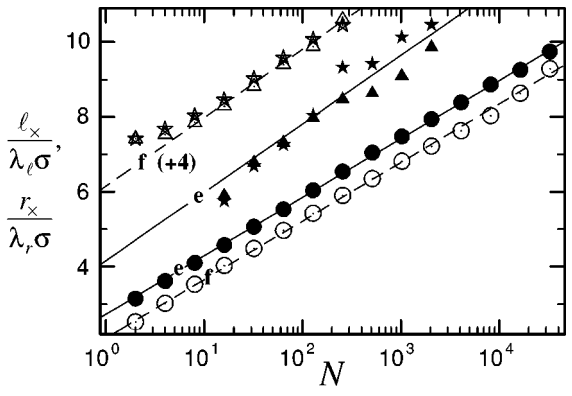

FIG. 3. Crossover lengths $\ell_\times(N)/\lambda_\ell\sigma$ and $r_\times(N)/\lambda_r\sigma$ versus N for electrons (**e**, filled symbols and continuous lines) and fractons (**f**, open symbols and dashed lines) on critical percolation clusters on the Cayley tree (circles) and on the square lattice (stars for ℓ space and triangles for r space) in a semilogarithmic plot. $\ell_\times(N)$ corresponds to those lengths ℓ, where the effective localization exponent $d_{\Psi,\ell}$ of $\Psi_N(\ell)$ intercepts with unity; the same definition holds for $r_\times(N)$. The values for λ_ℓ, λ_r, and σ have been determined from the distributions of the amplitudes (see Figs. 4, 6, and 8). The points for fractons on the square lattice have been shifted up by 4 units on the $\ell_\times$ axis. The straight lines are fits to the data with the form $\ell_\times(N)=\lambda_\ell\sigma(c_1+c_2\ln N)$, where $c_2=0.68$ for the Cayley tree and $c_2=0.79$ for the square lattice.

The second localization regime ranges from $\ell_1\approx\lambda_\ell$ up to a characteristic crossover length $\ell_\times(N)$, where $\Psi_N(\ell)$ departs from the common straight line. In this regime, we find a stretched exponential decay (''sublocalization'') with an effective exponent $d_{\Psi,\ell}\cong 0.62$ for both electrons and fractons. This sublocalization regime expands strongly as the number of configurations N increases. Note that in both the first and the second regime, $\Psi_N(\ell)$ is independent of N.

In the third regime, for $\ell>\ell_\times(N)$, self-averaging fails and $\Psi_N(\ell)$ depends explicitly on N. In the beginning of this regime, $d_{\Psi,\ell}$ is considerably larger than 1, corresponding to a faster than exponential decay (''superlocalization''). Only for extremely large ℓ values the simple exponential decay ($d_{\Psi,\ell}=1$) predicted in former work [1,16] is reached. For $N=1$, in contrast, simple exponential decay is observed already for ''relatively small'' values of ℓ, leaving out the intermediate localization regime completely.

To see how the crossover length $\ell_\times(N)$ increases with N, we have plotted $\ell_\times(N)$ versus $\log N$ in Fig. 3. Since $d_{\Psi,\ell}<1$ in the second regime and $d_{\Psi,\ell}>1$ in the third, the values of $\ell_\times(N)$ correspond to those lengths ℓ where $d_{\Psi,\ell}$ intercepts with unity. The straight lines in Fig. 3 indicate simple logarithmic dependences of $\ell_\times(N)$ on N. This logarithmic N dependence of the crossover length seems to be an inherent feature of strongly fluctuating quantities, which are characterized by a logarithmically broad distribution. It was first found in the context of random walks on self-similar structures [17], and occurs also in relaxation phenomena of the Kohlrausch type [23].

Figure 4 shows, for the case of electrons, typical examples of the distributions of ψ_n for various ℓ values from $\ell=15$ (a) to $\ell=500$ (d). For fractons, they have qualitatively the same shape. The figure shows that, for large ℓ, the histogram of the amplitudes ψ_n obeys a log-normal distribution,

$$H(x,\ell)=\frac{1}{\sqrt{\pi\sigma\ell/\lambda_\ell}}\exp\left[-\frac{(x-\ell/\lambda_\ell)^2}{\sigma\ell/\lambda_\ell}\right], \qquad (5)$$

where $x=-\ln\psi_n(\ell)\geqslant 0$. For the energy eigenvalue $E=1.7$ considered, the parameters $\lambda_\ell=6.5$ and $\sigma=2.7$ describe the distributions very well for sufficiently large ℓ. For fractons with $\omega^2=0.1$ we found $\lambda_\ell=5.8$ and $\sigma=3.1$. Since the fitting parameter λ_ℓ turns out to be independent of ℓ, it can be used as localization length. The insets of Fig. 4 show that the agreement between the numerical distribution and Eq. (5) becomes nearly perfect for larger ℓ values, indicating that the distribution follows Eq. (5) asymptotically (except for the irrelevant large x values). In the next section we show that this complex localization behavior occurs also in critical percolation structures in $d=2$ and $d=3$ which contain loops on all length scales.

IV. PERCOLATION CLUSTERS IN $d=2$ AND $d=3$

We consider electrons and fractons on (site)-percolation clusters in $d=2$ (square lattice) and $d=3$ (simple cubic lattice) at the percolation threshold. We have used the Leath method to generate large clusters with a maximum chemical length $\ell_{\max}=400$ and used the Lanczos method (see the Appendix) to determine the desired eigenfunctions of Eqs. (1)

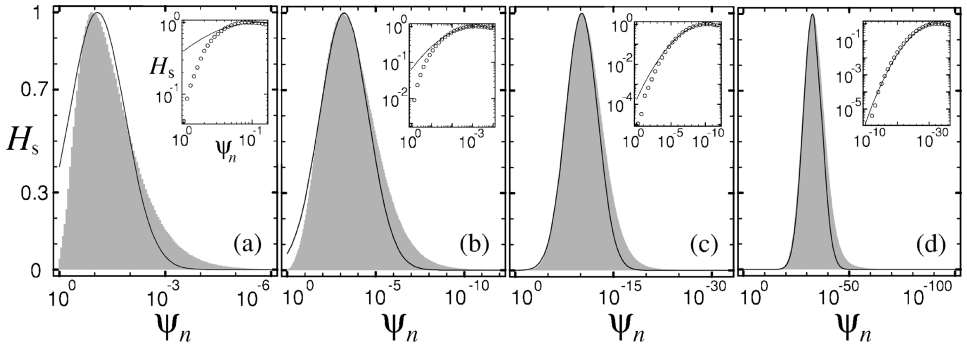

FIG. 4. Scaled histogram $H_s(x,\ell)=[\pi\sigma\ell/\lambda_\ell]^{1/2}H(x,\ell)$ of the amplitude values $\psi_n(\ell)=[\phi^*_{n,E}\phi_{n,E}]^{1/2}$ for electrons on critical percolation clusters on the Cayley tree at fixed chemical lengths ℓ from the center of localization: (a) $\ell=15$, (b) $\ell=50$, (c) $\ell=150$, and (d) $\ell=500$. The continuous lines represent Gaussian fits to the data according to Eq. (5) with the parameters $\lambda_\ell=6.5$ and $\sigma=2.7$. In the insets, the same distributions are shown in a logarithmic scale. 10^6 configurations were considered to calculate the distributions.

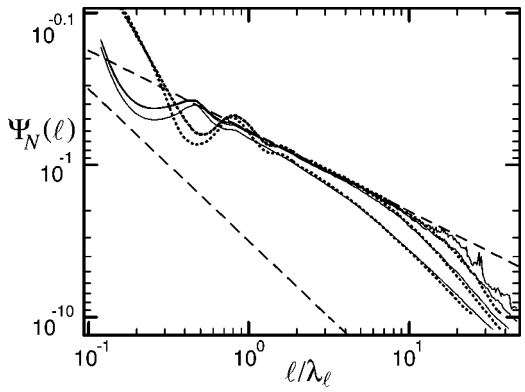

FIG. 5. ℓ space in $d=2$: The decrease of $\Psi_N(\ell)$ versus ℓ/λ_ℓ for electrons (continuous lines) and fractons (dotted lines) on critical percolation clusters in $d=2$ for several N values ($N=1$, 16, 256, 2048 for electrons and $N=1$, 16, 256 for fractons; from the bottom to the top). For electrons, 3×10^3 and for fractons 10^3 eigenfunctions on clusters of $\ell_{\max}=400$ shells were considered in the averaging procedure. As in Fig. 2, the values for λ_ℓ, $\lambda_\ell=8.4$ for electrons and $\lambda_\ell=10.6$ for fractons, have been determined from the corresponding distributions (see Fig. 6). In the intermediate regime the dashed straight line indicates a fit to the data with an effective localization exponent $d_{\Psi,\ell}=0.53$. The straight dashed line drawn below the numerical results has the slope $d_{\Psi,\ell}=1$ and is shown for comparison.

and (2). The iterative method applied to the Cayley tree could not be used here, since in $d=2$ and 3 the clusters have loops on all scales.

Figure 5 shows our numerical results for $\Psi_N(\ell)$ for electrons and fractons in $d=2$. The figure is analogous to Fig. 2, and it shows that again the localization behavior for electrons and fractons in topological space is quite complex, and very similar to the behavior observed for percolation on the Cayley tree. Again, we find three localization regimes for $N\gg1$: Superlocalization ($d_{\Psi,\ell}>1$) in the first regime $\ell<\lambda_\ell/2$,

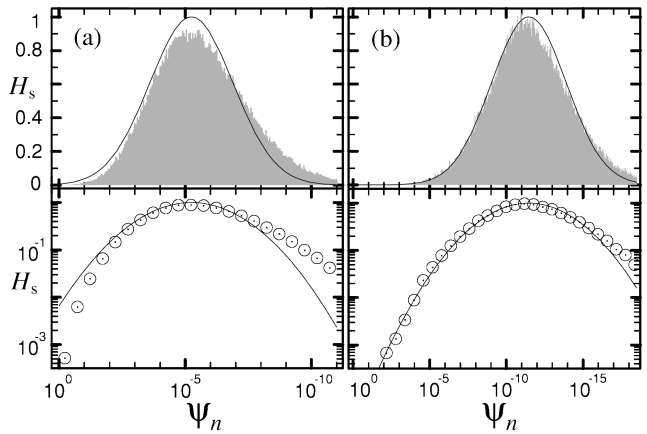

FIG. 6. ℓ space in $d=2$: Scaled histogram $H_s(x,\ell)=\times[\pi\sigma\ell/\lambda_\ell]^{1/2}H(x,\ell)$ of the amplitude values $\psi_n(\ell)$ for fractons on critical percolation clusters in $d=2$ at fixed chemical lengths ℓ from the localization center: (a) $\ell=128$ and (b) $\ell=280$. The continuous lines represent Gaussian fits to the data according to Eq. (5) with the parameters $\lambda_\ell=10.6$ and $\sigma=2.4$. In the lower parts of the figure the same distributions are shown in a logarithmic scale. 10^3 configurations were considered to calculate the distributions.

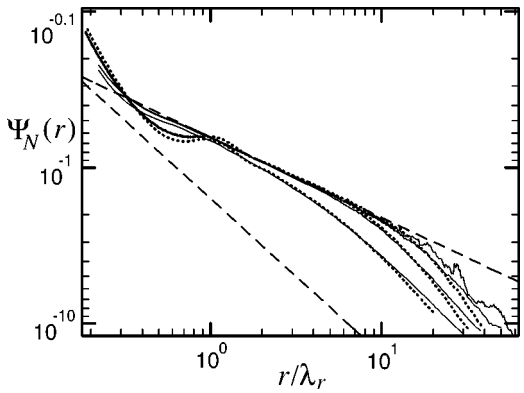

FIG. 7. r space in $d=2$: The decrease of $\Psi_N(r)$ versus r/λ_r for electrons (continuous lines) and fractons (dotted lines) on critical percolation clusters in $d=2$ for the same eigenfunctions and N values as in Fig. 5. The values for λ_r, $\lambda_r=4.5$ for electrons and $\lambda_r=5.4$ for fractons, have been determined from the corresponding distributions (see Fig. 8). In the intermediate regime, a dashed straight line indicates a fit to the data with an effective localization exponent $d_{\Psi,r}=0.52$. The straight dashed line drawn below the numerical results has the slope $d_{\Psi,r}=1$ and is shown for comparison.

sublocalization ($d_{\Psi,\ell}<1$) in the intermediate regime $\lambda_\ell<\ell<\ell_\times(N)$, and transient superlocalization with N dependence in the third regime $\ell>\ell_\times(N)$, converging to simple exponential localization ($d_{\Psi,\ell}=1$) for $\ell\to\infty$. In the intermediate regime, the effective sublocalization exponent $d_{\Psi,\ell}\cong0.53$ has approximately the same value for electrons and fractons. This value is significantly smaller than the one for the Cayley tree (where we found $d_{\Psi,\ell}\cong0.62$). As for the Cayley tree the crossover length $\ell_\times(N)$ (shown in Fig. 3) increases logarithmically with N, hence the regime of sublocalization becomes the dominant one for large values of N.

Figure 6 shows the histogram of the amplitudes ψ_n for fixed ℓ for fractons. The figure is analogous to Fig. 4 for the Cayley tree. The continuous lines correspond to the log-normal distribution function Eq. (5) with the parameters $\lambda_\ell=10.6$ and $\sigma=2.4$ for fractons ($\lambda_\ell=8.4$ and $\sigma=2.1$ for

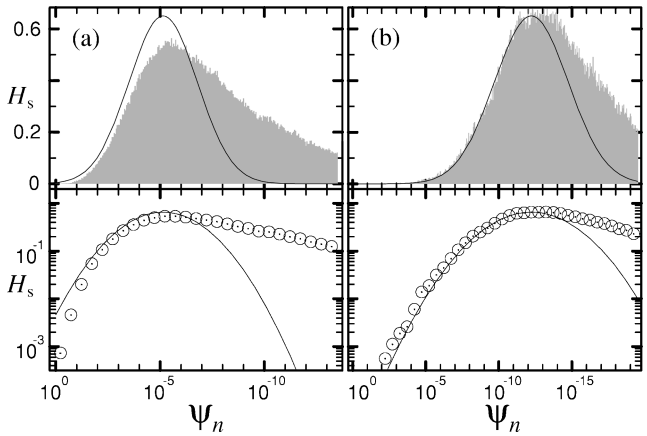

FIG. 8. r space in $d=2$: Scaled histogram $H_s(x,r)=\times[\pi\sigma r/\lambda_r]^{1/2}H(x,r)$ of the amplitude values $\psi_n(r)$ for fractons on critical percolation clusters in $d=2$ at fixed lengths r from the localization center: (a) $r=64$ and (b) $r=150$, corresponding to Fig. 6. The continuous lines represent Gaussian fits to the data according to Eq. (6) with the parameters $\lambda_r=5.4$, $\sigma=2.4$, and $A=0.65$.

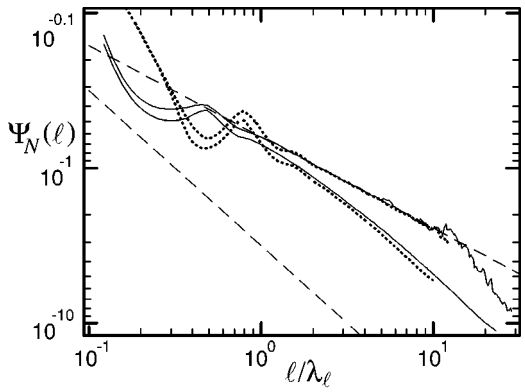

FIG. 9. ℓ space in $d=3$: The decrease of $\Psi_N(\ell)$ versus ℓ/λ_ℓ for electrons (continuous lines) and fractons (dotted lines) on critical percolation clusters in $d=3$ for two effective numbers of configurations: $N=1$ (bottom lines) and $N\approx 10^3$ (top lines). Approximately 10^3 eigenfunctions on clusters of $\ell_{\max}=250$ shells were considered in the averaging procedure. The values $\lambda_\ell=8.2$ and $\lambda_\ell=10.2$ are used for electrons and fractons, respectively. A dashed straight line indicates a fit to the data in the intermediate regime with an effective localization exponent $d_{\Psi,\ell}=0.59$. The straight dashed line drawn below the numerical results has the slope $d_{\Psi,\ell}=1$ and is shown for comparison.

electrons). We see again that, for large values of ℓ, the log-normal distribution fits the numerical distribution quite well, and we can anticipate that for sufficiently large ℓ values Eq. (5) becomes exact.

Next we consider localization in r space in $d=2$. Since the distribution of ψ_n is logarithmically broad in ℓ space, and $\Psi_N(\ell)$ depends on N, the analytical arguments mentioned in the Introduction cannot be applied here.

Figures 7 and 8 show our numerical results for the localization behavior of electrons and fractons in r space, which is very similar to the localization behavior in ℓ space (shown in Figs. 5 and 6) with nearly the same effective localization exponent ($d_{\Psi,r}\cong 0.52$) in the sublocalization regime. Also

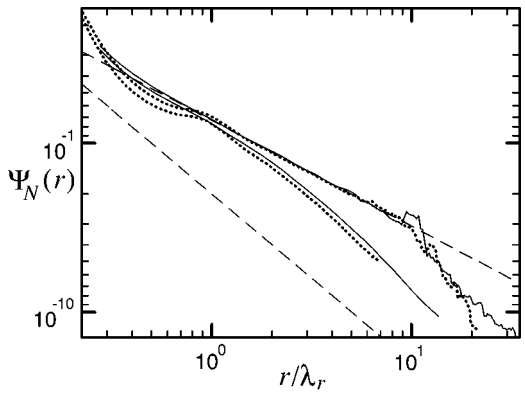

FIG. 10. r space in $d=3$: The decrease of $\Psi_N(r)$ versus r/λ_r for electrons (continuous lines) and fractons (dotted lines) in $d=3$ for the same eigenfunctions and N values as in Fig. 9. Here, the values $\lambda_r=3.6$ and $\lambda_r=4.4$ are used for electrons and fractons, respectively. In the intermediate regime, a dashed straight line indicates a fit to the data with an effective localization exponent $d_{\Psi,r}=0.63$.

the crossover length $r_\times(N)$ (Fig. 3) has the same simple logarithmic dependence on the number of configurations N that we found already in ℓ space.

The reason for this can be understood from the distribution of the values ψ_n, now for fixed distance r from the localization center. Two examples of the distribution are shown in Fig. 8; the figure corresponds to Fig. 6 for the ℓ space. The continuous lines represent fits to the left part of the histogram by the log-normal distribution

$$H(x,r)=\frac{A}{\sqrt{\pi\sigma r/\lambda_r}}\exp\left[\frac{-(x-r/\lambda_r)^2}{\sigma r/\lambda_r}\right] \tag{6}$$

[similar to $H(x,\ell)$ in Eq. (5)] with the parameters $\lambda_r=5.4$, $\sigma=2.4$, and $A=0.65$ for fractons ($\lambda_r=4.5$ and $\sigma=2.1$ for electrons). The right part corresponds to very small values of ψ_n, and therefore is not essential for the calculation of arithmetical averages. Since the histogram deviates from the log-normal form in this irrelevant area, we included an additional factor A into our ansatz Eq. (6) in order to fit the left part of the histogram. Since the factor A is only weakly r dependent and close to unity, it does not influence the r dependence of $\Psi_N(r)$. The relevant left part of the distribution, which corresponds to large values of ψ_n, can be fitted well by Eq. (6). This results in a localization behavior in r space similar to the behavior in ℓ space, and explains the resemblance of Figs. 5 and 7.

Figures 9 and 10 show our numerical results for $\Psi_N(\ell)$ and $\Psi_N(r)$ for electrons and fractons on site percolation clusters in $d=3$. Again, we discover a decay similar to that in $d=2$ and on the Cayley tree, with a pronounced intermediate (sublocalization) regime for $N\gg 1$. The effective localization exponents $d_{\Psi,\ell}\cong 0.59$ and $d_{\Psi,r}\cong 0.63$, hold over more than one order of magnitude in ℓ and r and are equal within the error bars. The values are similar to $d_{\Psi,\ell}\cong 0.62$, we obtained on the Cayley tree, and larger than in $d=2$. Again the typical average for one configuration, $\Psi_1(\ell)$, shows simple exponential localization asymptotically.

V. THEORETICAL DESCRIPTION

Since we know analytically the distribution of dominating amplitudes $\psi_n(\ell)$ at chemical distances $\ell\gg\lambda_\ell$, we can calculate $\Psi_N(\ell)$ for large ℓ by simple integration. In particular, we can obtain $\Psi_N(\ell)$ in the asymptotic regime which was not accessible numerically. We can also estimate the way $\Psi_N(\ell)$ depends on N. The calculation is valid for both electronic wave functions and fractons on critical percolation clusters on the Cayley tree and in $d=2$ (and $d=3$), since the same log-normal distribution $H(x,\ell)$ [Eq. (5)] fits in all these cases (only the two parameters λ_ℓ and σ have to be adapted).

If we average over all configurations, the resulting quantity $\Psi_\infty(\ell)$ is related to $H(x,\ell)$ by

$$\Psi_\infty^2(\ell)=\int_0^\infty e^{-2x}H(x,\ell)dx. \tag{7}$$

For a *finite* number N of configurations, the total number of sites at distance ℓ from the localization center is identical to $N\cdot\langle N_\ell\rangle$ with $\langle N_\ell\rangle=a\ell^{d_\ell-1}$ ($a=$const). Here, d_ℓ is the

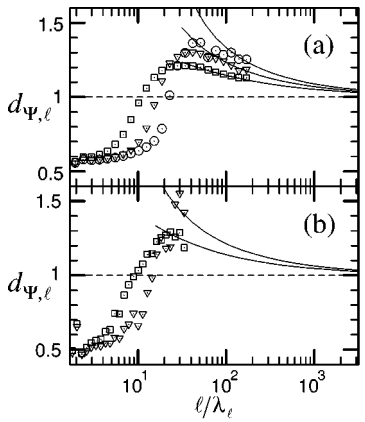

FIG. 11. Effective localization exponents $d_{\Psi,\ell}$ versus ℓ/λ_ℓ for (a) electrons on the Cayley tree and (b) fractons in $d=2$. The symbols are from the numerical calculations for $N=16$ (squares), $N=256$ (triangles), and [only in (a)] $N=4096$ (circles). The lines represent the analytical result for the large-ℓ regime [Eq. (11) with $N=16$, 256, and 4096].

topological (or chemical) dimension of the percolation clusters, which describes how the number of cluster sites (the ''mass'' M) scales with ℓ, $M(\ell)\sim\ell^{d_\ell}$. Its values are $d_\ell\cong 1.678$ (1.84) for percolation in $d=2$ (3), and $d_\ell=2$ for the Cayley tree. Clearly, those values of $x=-\ln\psi_n(\ell)$ with a too small probability ($H(x,\ell)<1/N\langle N_\ell\rangle$) are unlikely to occur in N typical configurations, and the condition

$$H(x_{\min},\ell)=1/(N\langle N_\ell\rangle)=1/(aN\ell^{d_\ell-1}) \tag{8}$$

determines a lower cutoff value

$$x_{\min}(\ell,N) = \max\{0,\ell/\lambda_\ell-\sqrt{(\sigma\ell/\lambda_\ell)\ln[aN\ell^{d_\ell-3/2}\sqrt{\lambda_\ell/(\pi\sigma)}]}\}, \tag{9}$$

which replaces the lower integration bound in Eq. (7) for finite N. Hence, for finite N, Eq. (7) becomes

$$\Psi_N^2(\ell)=\int_{x_{\min}(\ell,N)}^{\infty} e^{-2x}H(x,\ell)dx. \tag{10}$$

The integration can be performed straightforwardly and gives

$$\Psi_N(\ell)\cong\frac{1}{\sqrt{2}}\exp\left[\frac{(\sigma/2-1)\ell}{\lambda_\ell}\right]\left(1-\mathrm{erf}\left\{\sqrt{\frac{\sigma\ell}{\lambda_\ell}}-\sqrt{\ln[aN\ell^{d_\ell-3/2}\sqrt{\lambda_\ell/(\pi\sigma)}]}\right\}\right)^{1/2}. \tag{11}$$

Equation (11) is supposed to be rigorous for sufficiently large ℓ values ($\ell\gg\lambda_\ell$), where the distribution of ψ_n is described by the log-normal distribution $H(x,\ell)$. The typical average $\Psi_1(\ell)$ can be deduced by setting $N=1$.

In Fig. 11 we compare the effective exponents $d_{\Psi,\ell}$ for electrons on percolation clusters on the Cayley tree and in $d=2$ derived from Eq. (11) with our numerical results for several N. As predicted, Eq. (11) describes the localization behavior of $\Psi_N(\ell)$ in the asymptotic large ℓ regime [$\ell\gg\ell_\times(N)$].

Equation (11) is not valid for small ℓ values, for which the lower integration limit $x_{\min}(\ell,N)$ in Eq. (10) tends to zero. For sufficiently small ℓ values, the real distribution of ψ_n deviates from the log-normal distribution $H(x,\ell)$ for small x values corresponding to large ψ_n, as can be seen in Figs. 4 and 6. In this case, the log-normal approximation is inappropriate, and therefore cannot yield exact results for $\Psi_N(\ell)$.

Despite this, the log-normal approximation can be used for obtaining a qualitative picture of $\Psi_N(\ell)$ at intermediate ℓ values, where $x_{\min}(\ell,N)=0$. It can be shown that the integration of Eq. (7) yields an effective localization exponent $d_{\Psi,\ell}\approx 0.6$, which quite nicely agrees with the exponents we found numerically in the intermediate localization regime $\lambda_\ell<\ell<\ell_\times(N)$. Since the number of configurations N does not appear in Eq. (7), it is evident that $\Psi_N(\ell)$ does not depend on N in this regime, in agreement with our numerical finding.

Furthermore, we can obtain a qualitative description of the logarithmic N dependence of $\ell_\times$, if we identify $\ell_\times(N)$ with the largest distance ℓ for which the condition $x_{\min}(\ell,N)=0$ holds. This yields [with Eq. (9)]

$$\ell_\times(N)=\lambda_\ell\sigma[2\ln N+(2d_\ell-3)\ln\ell_\times(N) - \ln(a^2\pi\sigma/\lambda_\ell)]/2, \tag{12}$$

which is an implicit equation for $\ell_\times(N)$. As described above, we cannot expect to find a quantitative agreement here, since the log-normal distribution function $H(x,\ell)$ does not fit well for very small x. For $N\gg 1$ Eq. (12) reduces to

$$\ell_\times(N)\approx\lambda_\ell\sigma\ln N + \lambda_\ell\sigma\ln[\lambda_\ell^{d_\ell-1}\sigma^{d_\ell-2}(\ln N)^{d_\ell-3/2}/(a\sqrt{\pi})], \tag{13}$$

with a logarithmic dependence on N similar to our numerical results, since the second term depends weakly on N (because $1.68\leqslant d_\ell\leqslant 2$).

It is remarkable that by this simple approach, the essential features of the localization phenomenon, sublocalization in the intermediate regime, crossover to superlocalized behavior (that depends on the number of configurations N), and final approach to simple exponential behavior, are reproduced.

It is important to note that Eq. (11) enables us to determine the behavior of $\Psi_N(\ell)$ also for those values of N and ℓ that are not numerically accessible. Figure 11 shows $d_{\Psi,\ell}$ obtained from Eq. (11) for four values of N and very large ℓ values. For $\ell\approx 10^3\lambda_\ell$, which is far above the numerically accessible range, we find $d_{\Psi,\ell}\approx 1.08$ (for $N=10^3$ in the third regime). Thus, the asymptotic value $d_{\Psi,\ell}=1$ will only be reached for extremely large ℓ, where $\Psi_N(\ell)$ is smaller than 10^{-100}. It is remarkable that for a macroscopically large number of configurations $N\approx 10^{23}$ the crossover length $\ell_\times(N)$ remains finite [$\ell_\times(10^{23})\approx 10^3$]. Thus, the third (superlocalization) regime with the N dependence of the aver-

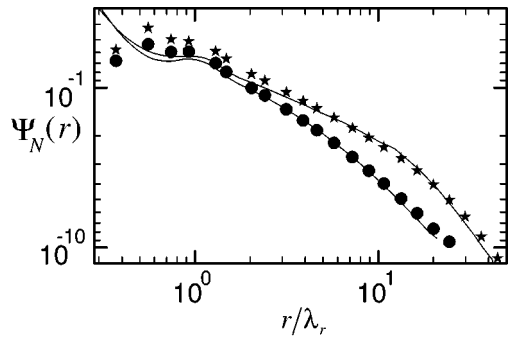

FIG. 12. r space in $d=2$: Comparison of the directly determined $\Psi_N(r)$ versus r/λ_r for fractons on critical percolation clusters in $d=2$ (lines) and the $\Psi_N(r)$ calculated from $\Psi_N(\ell)$ by numerical integration of Eq. (14) (symbols). The data for two different numbers of configurations $N=1$ (circles) and $N=256$ (stars) are included.

aged eigenfunctions is still present even for a macroscopically large number of configurations, although its beginning moves to large ℓ values and the second (sublocalization) regime becomes most important.

Our theoretical description is also appropriate in r space, even though the distribution of ψ_n for fixed r has a more complicated shape than in ℓ space. But the log-normal distribution [Eq. (6)] fits the left shoulder of the distribution of $\psi_n(r)$ quite well. So the calculations in this section can be transferred to r space simply by replacing ℓ by r, λ_ℓ by λ_r, and d_ℓ by the fractal dimension d_f in Eqs. (7) to (13). From this approach, since the widths σ of the distributions turn out to be the same, if only the left shoulder of the distributions is taken into account in the fitting procedure, we obtain the same localization exponent in ℓ and in r space, $d_{\Psi,\ell}=d_{\Psi,r}$. We also confirmed this numerically within the error bars.

It has been shown in Refs. [1,17], see also [18], that $\Psi_N(\ell)$ and $\Psi_N(r)$ are related by the convolution

$$\Psi_N(r)=\int_{\ell_{\min}(r,N)}^{\infty}\phi(\ell|r)\Psi_N(\ell)d\ell, \tag{14}$$

if the distribution of the amplitude values ψ_n at fixed chemical distance ℓ is sufficiently narrow. Here, $\ell_{\min}(r,N)$ is defined as the minimal path distance connecting two cluster sites at distance r, and the structure function $\phi(\ell|r)$ is defined as the probability that two cluster sites at spatial distance r are separated by a chemical distance between ℓ and $\ell+d\ell$, divided by $d\ell$. $\phi(\ell|r)$ is a well known single hump function (see, e.g., [10]).

It is interesting to note that even though the basic assumption leading to Eq. (14) (narrow distribution of ψ_n at fixed ℓ) is strongly violated here, the equation can nevertheless serve as a very good approximation. This is shown in Fig. 12 for fractons on critical percolation clusters in $d=2$ for $N=1$ and $N=256$. The symbols represent the data points obtained by numerical integration of Eq. (14), the lines are the numerical results shown already in Fig. 7. The agreement between data points and lines is satisfactory.

VI. CONCLUSION

We have investigated the mean amplitudes of electronic wave functions and fractons on percolation clusters at criticality. We found that the typical averages over N configurations in ℓ and r space, $\Psi_N(\ell)$ and $\Psi_N(r)$, decay in a rather complicated, but surprisingly similar way. In the intermediate localization regime, which expands logarithmically with the number of configurations N, localization is characterized by effective localization exponents considerably lower than 1. In the asymptotic regime, the mean amplitudes depend logarithmically on N. The exponents governing localization in both regimes are identical (within the error bars) for electrons and fractons.

Further research work is needed in order to see, for example, how the sublocalization regime influences the thermally activated hopping conductivity, or if the N dependence of the amplitudes in the asymptotic regime leads to an anomalous size dependence of physical quantities. A question of great interest concerns the localization behavior of fractons and electrons above p_c. It is believed that fractons show transitions from localized to extended behavior in $d=2$ (see, e.g., [10]), while electrons do not [3]. This seems to be contradicting to our results at the percolation threshold, where the amplitudes of electronic wave functions and fractons can hardly be distinguished.

ACKNOWLEDGMENTS

We like to thank our colleague Dr. H.E. Roman for many useful discussions. We are very much indebted to him for bringing Ref. [24] to our attention and for explaining to us the numerical algorithm used therein. This work was supported by the Deutsche Forschungsgemeinschaft.

APPENDIX: NUMERICAL METHODS

In this appendix we present details of the calculation of the eigenfunctions we performed for Eqs. (1) and (2) and briefly describe the algorithm we used for the Cayley tree structures. Throughout the whole paper we considered electronic eigenfunctions with eigenvalues $E=1.7\pm0.05$ and vibrational excitations with frequency eigenvalues $\omega^2=0.1\pm0.01$. Since the exact eigenvalues are not the same in every cluster configuration, we could not stick to a fixed value of E respectively ω, but we had to consider solutions with eigenvalues in the small intervals. The values $E=1.7$ and $\omega^2=0.1$ were chosen in order to obtain electrons and fractons with similar localization lengths. Some special values (e.g., $E^2=0,1,2$ for electrons) had to be avoided, because strong degeneration and energy dependencies of the localization lengths on E occur there [21,6].

For $d=2$ and $d=3$, the eigenfunctions were calculated with Lanczos' algorithm [25] on clusters with up to 4×10^4 sites with quadruple precision (except for the fractons in $d=3$, where only double precision was used to save computer time). For the Cayley tree, the percolation structures are loopless, and this enabled us to construct a considerably faster, iterative algorithm for the calculation of a single eigenfunction in a given configuration. The algorithm extends earlier work [24] on the tight-binding equation for the

Anderson model in $d=1$ to the Cayley tree. Here, we present only a brief description of the iterative algorithm for a Cayley tree with coordination number $z=3$. For a detailed description, see Ref. [26].

In the first step, we assign the value $\phi_n=1$ to all perimeter sites n (we denote electron *and* fracton eigenfunctions by ϕ in this description for simplicity). We start with the sites at maximum chemical distance $\ell_{\max}$ from the origin, use the desired eigenvalue (energy E or frequency ω) as input, and employ Eq. (1) [respectively Eq. (2)] for the sites n at $\ell_{\max}$ to determine the values ϕ_m assigned to the sites m at chemical distance $\ell=\ell_{\max}-1$. In the next step, these values are used as input to calculate the values of ϕ_m at chemical distance $\ell=\ell_{\max}-2$ from the center, and so on. In the $\ell_{\max}$th step, finally, we determine the value of ϕ_0.

A problem occurs at the branching points, where a site m at chemical distance ℓ has not one, but two nearest neighbor sites n at chemical distance $\ell+1$, since then the procedure assigns two—possibly different—values $\phi_{(m,1)}$ and $\phi_{(m,2)}$ to site m. This ambiguity can be eliminated simply by multiplying all ϕ_n values in the second branch by $\phi_{(m,1)}/\phi_{(m,2)}$, such that both nearest neighbor sites at $\ell+1$ give the same value $\phi_{(m,1)}$ for the branching site m. This procedure is possible, since the branches are not interconnected above site m and Eqs. (1) and (2) are linear equations.

To determine the values of ϕ_n at all cluster sites, we employed Eq. (1) [respectively Eq. (2)] for all sites n with chemical distance $\ell \geqslant 1$. The final equation for site 0, which remains to be considered, is only satisfied if ϕ is an eigenfunction, or equivalently, if E (respectively ω) is an eigenvalue. If this is not the case, the whole procedure is repeated from the beginning with a different starting value of E (respectively ω), until the final equation for site $n=0$ is satisfied within the required accuracy. In practice, the problem reduces to searching a zero of the equation for the site at $n=0$, which is achieved when the relative error in this equation is smaller than a limit ϵ. In our calculations we used $\epsilon=10^{-10}$. Finally, the eigenfunction ϕ_n is ''normalized'' so that $|\phi_{n_0}|^2=1$ for the localization center site n_0.

We like to note that this algorithm can be used quite generally for the calculation of eigenfunctions of linear equations with nearest neighbor coupling on loopless structures. The main advantages of the algorithm, compared with the Lanczos algorithm, are its speed and the fact that much larger systems can be investigated. Also, double precision is sufficient for the calculation of the localized eigenfunctions even down to regions with amplitudes smaller than 10^{-100}.

[1] A. Bunde, H.E. Roman, St. Russ, A. Aharony, and A.B. Harris, Phys. Rev. Lett. **69**, 3189 (1992).

[2] B. Kramer and A. MacKinnon, Rep. Prog. Phys. **56**, 1469 (1993).

[3] A. Mookerjee, I. Dasgupta, and T. Saha, Int. J. Mod. Phys. B **9**, 2989 (1995).

[4] T. Nakayama, K. Yakubo, and R.L. Orbach, Rev. Mod. Phys. **66**, 381 (1994).

[5] I. Chang, Z. Lev, Y. Meir, A.B. Harris, J. Adler, and A. Aharony, Phys. Rev. Lett. **74**, 2094 (1995).

[6] R. Berkovits and Y. Avishai, Phys. Rev. B **53**, R16125 (1996).

[7] G. Deutscher, Y.-E. Levy, and B. Souillard, Europhys. Lett. **4**, 577 (1987); A.B. Harris and A. Aharony, *ibid.* **4**, 1355 (1987).

[8] D. van der Putten, J.T. Moonen, H.B. Brom, J.C.M. Brokken-Zijp, and M.A.J. Michels, Phys. Rev. Lett. **69**, 494 (1992); **70**, 4161 (1993); A. Aharony, A.B. Harris, and O. Entin-Wohlman, *ibid.* **70**, 4160 (1993).

[9] P. Mandal, A. Neumann, A.G.M. Jansen, P. Wyder, and R. Deltour, Phys. Rev. B **55**, 452 (1997).

[10] *Fractals and Disordered Systems*, edited by A. Bunde and S. Halvin, 2nd ed. (Springer Verlag, Heidelberg, 1996).

[11] D. Stauffer and A. Aharony, *Introduction to Percolation Theory*, 2nd ed. (Taylor & Francis, London, 1992).

[12] Y.-E. Levy and B. Souillard, Europhys. Lett. **4**, 233 (1987).

[13] P. de Vries, H. de Raedt, and A. Lagendijk, Phys. Rev. Lett. **62**, 2515 (1989); H.E. Roman, St. Russ, and A. Bunde, *ibid.* **66**, 1643 (1991).

[14] C.J. Lambert and G.D. Hughes, Phys. Rev. Lett. **66**, 1074 (1991).

[15] A. Bunde and H.E. Roman, Philos. Mag. B **65**, 191 (1992).

[16] A. Aharony and A.B. Harris, Physica A **191**, 365 (1992).

[17] A. Bunde and J. Dräger, Phys. Rev. E **52**, 53 (1995); J. Dräger and A. Bunde, *ibid.* **54**, 4596 (1996).

[18] S. Havlin and D. Ben-Avraham, Adv. Phys. **36**, 695 (1987).

[19] The maximum is always well defined, since we considered double or even quadrupole precision values. Quasidegenerate states having more than one localization center did not occur.

[20] J. Dräger, St. Russ, and A. Bunde, Europhys. Lett. **31**, 425 (1995).

[21] S. Kirkpatrick and T.P. Eggarter, Phys. Rev. B **6**, 3598 (1972).

[22] S. Alexander and R. Orbach, J. Phys. (Paris) Lett. **43**, L625 (1982).

[23] A. Bunde, S. Havlin, J. Klafter, G. Gräff, and A. Shehter, Phys. Rev. Lett. **78**, 3338 (1997).

[24] H.E. Roman and C. Wiecko, Z. Phys. B **62**, 163 (1986).

[25] C. Lanczos, J. Res. Natl. Bur. Stand. **45**, 255 (1950); J. Cullum and R. Willoughby, *Lanczos Algorithms for Large Symmetric Eigenvalue Computations* (Birkhaeuser, Boston, 1985).

[26] J. W. Kantelhardt, Diploma thesis (in German), University of Gießen, 1996 (unpublished).